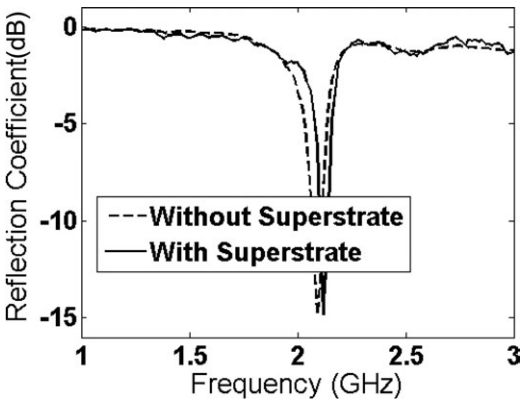

Figure 5 The experimental reflection coefficient of the array with and without the superstrate

analytical method and CST. The proposed analytical technique requires only 12 min and 370 megabytes of RAM using MATLAB, while the CST simulations for the same structure require about 8 h and 6 gigabytes of RAM when 45 cells/wavelength with total of 4.6 M mesh-cells were used for the entire structure. However, the analytical technique as presented in this work is not capable of determining the input impedance. The directivity enhancement in the broadside direction of the antenna array due to the superstrate is predicted by CST and the analytical method to be 3.4 and 1.7 dB [6], respectively. This difference is due to the geometrical approximations taken into account in the analytical method to simplify the simulation procedure such as the infinite ground plane assumption. The measured reflection coefficient (S_{11}) of the antenna with and without the superstrate is depicted in Figure 5. It can be observed that the antenna in both the cases radiates good and is matched with the 50 Ω line. A slight change in the resonant frequency and the antenna bandwidth is observed because of the change in the near field properties of the antenna when the superstrates is added.

4. CONCLUSION

An enhanced-gain experimental antenna array system is proposed. The gain enhancement is achieved by covering the 2.18 GHz 4 × 1 corporate-fed microstrip patch array with a magneto-dielectric metamaterial superstrate that has an effective refractive index of 9.18. The directivity radiation patterns of 4 × 1 linear microstrip array covered with an artificial magneto-dielectric superstrate are calculated by a fast and accurate analytical method. The method is based on the reciprocity theorem and the transmission line modeling of the antenna-superstrate structure. The radiation patterns results are validated with the full-wave simulator CST and measurements, good agreement was achieved. The proposed formulation requires only 2.5% of the time acquired by full-wave analysis. The superstrate-based directivity enhancement method can be used in commercial antennas to combat some of the downsides of the existing systems such as gain decrease due to surface waves and dielectric losses.

REFERENCES

1. D.R. Jackson and N.G. Alexopoulos, Gain enhancement methods for printed circuit antennas, IEEE Trans Antennas Propagat AP-33 (1985), 976–987.
2. S. Maslovski, P. Ikonen, I. Kolmakov, and S. Tretyakov, Artificial magnetic materials based on the new magnetic particle: metasolenoid, Prog Electromagn Res 54 (2005), 61–81.
3. N.G. Alexopoulos, C.A. Kyriazidou, and H.F. Contopanagos, Effective parameters for metamorphic materials and metamaterials through a resonant inverse scattering approach, IEEE Trans Microwave Theory Tech 55 (2007), 254–267.
4. H. Attia, L. Yousefi, M.M. Bait-Suwailam, M. Said Boybay, and O.M. Ramahi, Enhanced-gain microstrip antenna using engineered magnetic superstrates, IEEE Antenna Wireless Propagat Lett 8 (2009), 1198–1201.
5. C. Balanis, Antenna theory: Analysis and design, 2nd ed., Wiley, New York, NY, 1997.
6. H. Attia, O. Siddiqui, and O.M. Ramahi, Artificial magneto-superstrates for gain and efficiency improvement of microstrip antenna arrays, In: Proceeding of the 28th PIER Symposium, Cambridge, MA, July 2010, pp. 878–881.

COMPACT SLOT ANTENNA WITH BAND-NOTCH CHARACTERIZATION FOR MULTIFUNCTIONAL COMMUNICATION SYSTEMS

A. C. Shagar[1] and R. S. D. Wahidabanu[2]
[1] Department of Electronics and Communication Engineering, Anna University of Technology-Tiruchirappalli, Tamilnadu, India; Corresponding author: shagar_einstein@rediffmail.com
[2] Department of Electronics and Communication Engineering, Anna University of Technology-Coimbatore, Tamilnadu, India

Received 15 May 2012

ABSTRACT: *In this article, a compact design and construction of a wide slot antenna with band-notch characteristics of size 28 × 32 × 1.6 mm is proposed and developed for multifunctional communication systems. Detailed simulations and experimental investigations are performed to understand its behavior and to optimize for 2.4 GHz WLAN and ultrawideband operations. An FR4 substrate with a thickness of 1.6 mm and relative permittivity of 4.4 is used to design the antenna. The antenna has a modified rectangular stub with coplanar waveguide feed technique. The modified rectangular shaped stub excites similar shaped slot in the ground plane, which improves the impedance matching from 2.1 to 30 GHz for VSWR less than 2. In addition, notch band characteristics in the 5.1–5.9 GHz band are achieved by making a slot on the tuning stub. Numerical and experimental results are reported to access the performance of the antenna in terms of impedance matching and radiation characteristics. A good agreement is found between the simulation and experimental results.* © 2012 Wiley Periodicals, Inc. Microwave Opt Technol Lett 55:218–223, 2013; View this article online at wileyonlinelibrary.com. DOI 10.1002/mop.27231

Key words: *co-planar waveguide; new slot antenna; WLAN and ultrawideband operation; modified rectangular stub and notch-band*

1. INTRODUCTION

In 2002, the Federal Communications Commission of the United State officially released the regulation for Ultrawideband (UWB) technology [1]. UWB communication antennas require low VSWR, linear phase, constant group delay and constant gain over entire operating frequency band [2]. In addition to these requirements, it is also required to use antennas of small size to reduce the total size of the communication systems. Based on the above requirements, many antenna configurations including planar monopole and dipole antennas have been developed so far. In these antennas, a variety of shapes and bandwidth enhancement techniques has been studied. Several shapes such as diamond [3], ring [4], bow-tie [5], elliptical [6], and square shapes [7] have been proposed to satisfy UWB specifications.

Slot antennas are currently under consideration for use in UWB systems because they have attractive advantages such as low profile, light weight, ease of fabrication and wide frequency bandwidth. Printed slot antennas are able to radiate omnidirectional radiation pattern with large bandwidth. This type of antenna can be realized using microstrip line or CPW feeding structures. For narrowband and wideband operations, the slot antenna takes various configurations such as rectangle [8], circle [9], triangle [10], and arc-shape [11], and so forth. In microstrip-fed slot antennas, etching is required on both sides of the dielectric substrate. Therefore, it leads to misalignment error. Moreover, microstrip line is not compatible with monolithic integrated circuits [12–14]. Because of the above limitations, various printed slot antennas fed by a coplanar waveguide (CPW) have been studied extensively. In Ref. 15, a CPW-fed rectangular slot antenna with a U-shaped tuning stub is proposed for wideband applications. It provides a wide bandwidth of 110% with gain variation from 1.9 to 5.1 dBi. Thus, it covers the entire UWB range of frequencies. But, the antenna size is too big, that is, 100 × 100 mm^2. In Ref. 16, UWB circular CPW-fed slot antenna has been proposed for the 3.1–10.6 GHz band operation. The antenna is comprised of circular stub that excites similar shaped slot. The same slot shape was excited by a U-shaped tuning stub in Ref. 17. The above referred antennas possess the lowest operating frequency at about 3 GHz, which makes them not suitable for multifunctional communication systems such as 2.4 GHz WLAN (2.4–2.484 GHz) and UWB systems. A CPW fed slot antenna which can be used for 2.4 GHz WLAN and UWB operations is not widely studied.

In this article, a wideband CPW fed slot antenna with 5 GHz notch band for applications in 2.4 GHz WLAN and UWB systems is proposed. Using modified rectangular stub that excites similar shaped slot in the ground plane, a broad impedance bandwidth for 2.4 GHz WLAN and UWB is easily obtained. For the band-notched operation covering (5.15–5.825 GHz) WLAN band, a slot is embedded on the tuning stub. By adjusting the length of the slot, the desired band-notched function is realized. Experimental and simulated results of the constructed prototype are presented.

2. ANTENNA STRUCTURE AND DESIGN

Figure 1 shows the geometry of the proposed slot antenna and a Cartesian coordinate system. The substrate used for this design

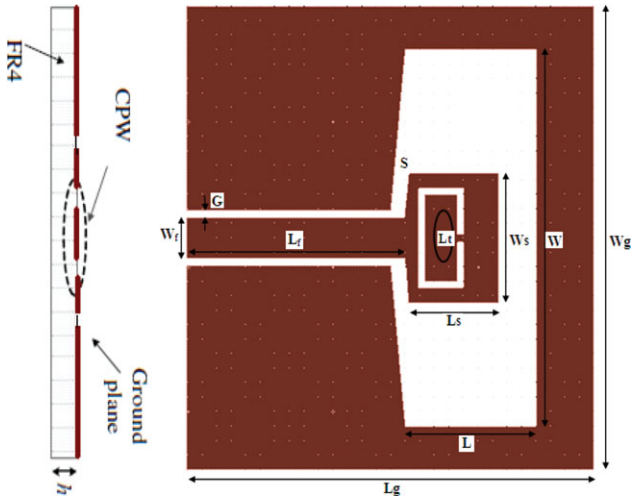

Figure 1 Geometry of the proposed antenna. [Color figure can be viewed in the online issue, which is available at wileyonlinelibrary.com]

TABLE 1 Optimal Design Parameters of the Antenna

Parameters	L_g	W_g	L	W	L_f	W_f	G	S	L_s	W_s	L_t
Optimum values (mm)	28	32	9.0	26	15	2.8	0.5	1.0	6.2	9.0	17.5

is FR4 with relative permittivity of 4.4 and thickness of $h = 1.6$ mm. Dimension of the ground plane is taken to be $L_g \times W_g$ mm. The antenna is located in y–z plane and the normal direction is parallel to x-axis. As illustrated in the figure, a CPW feed is used to excite the antenna. The CPW feed has a signal strip of thickness "W_f" and a gap of distance "G" between the signal strip and the coplanar ground plane. The characteristic impedance of the CPW feed line is 50 Ω. By choosing a suitable stub shape, slot shape and tuning their dimensions, the desired operating bandwidth is obtained in our design. Therefore, a modified rectangular stub is connected at the end of the CPW feed line and a similar shaped slot with dimension $W \times L$ mm is etched in the ground plane to achieve wide bandwidth for the proposed antenna. The CPW feed with modified rectangular stub strongly influences the performances of wide slot antenna. Moreover, the size of the feed is tuned such that it can occupy about one third of the slot size for optimum performance.

To implement notch band antenna design, a slot is embedded on the tuning stub. The length of the slot is varied to obtain the desired notch band function. Indeed, the slot introduced inside the tuning stub destroys the surface current on the ground plane so that the antenna makes nonresponsive at the notched frequency band. The optimum value of the slot length is $L_t = 17.5$ mm, which is found to be nearly equal to the quarter wavelength at notch band center frequency, that is, 5.5 GHz. This is obtained using the equation

$$\lambda/4 = c/4f\sqrt{\varepsilon_{\text{eff}}}$$

where,

$$\varepsilon_{\text{eff}} = (\varepsilon_r + 1)/2\varepsilon_r$$

The distance between the ground plane and stub (S) is taken to be 1.0 mm to couple more energy between the feed line and the slot in the ground plane. Hence, the modified rectangular tuning stub along with the slot is the basis of the proposed antenna. The detailed dimensions of the proposed antenna are given in Table 1.

A parametric study, which helps to investigate the effects of the different parameters on the impedance bandwidth, was conducted to optimize the antenna parameters. In the parametric study, one parameter is varied keeping all other parameters constant.

2.1. Effect of Stub Parameters

A wide slot is used in the ground plane of the antenna so that a high level of electromagnetic coupling can be achieved between the feed line and the slot. The coupling property and hence the operating bandwidth depends upon the feed shape. Therefore, the size of the CPW tuning stub can be adjusted to improve the impedance matching for the proposed antenna. Good impedance matching is achieved by tuning the length (L_s) and width (W_s) of the modified rectangular stub. This is evident from the simulated VSWR curves of the CPW fed slot antenna for various values of stub length (L_s) and stub width (W_s) as in Figures 2(a) and 2(b). From the figures, it is seen that the resonant frequency

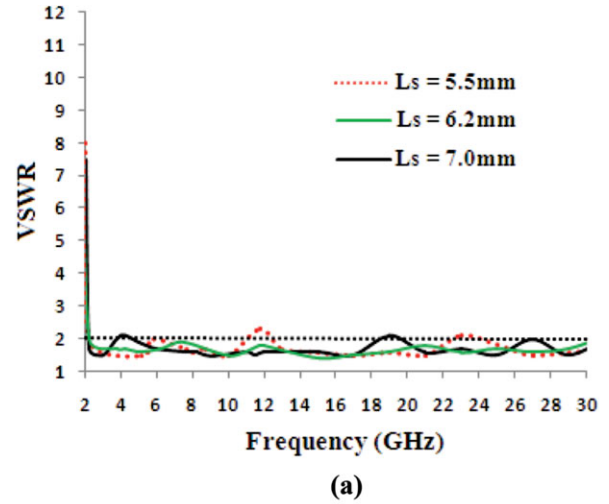

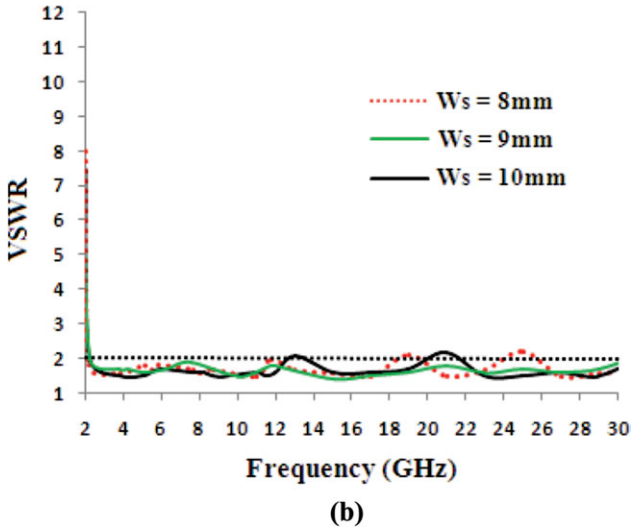

Figure 2 VSWR values of the antenna in terms of (a) L_s and (b) W_s. [Color figure can be viewed in the online issue, which is available at wileyonlinelibrary.com]

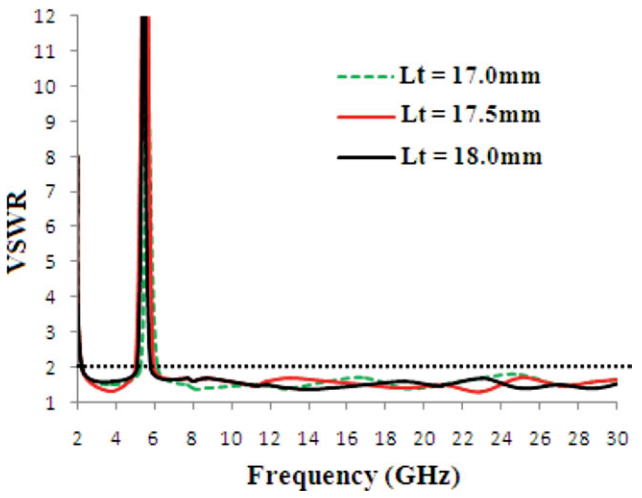

Figure 3 VSWR values of the proposed antenna in terms of slot length "Lt." [Color figure can be viewed in the online issue, which is available at wileyonlinelibrary.com]

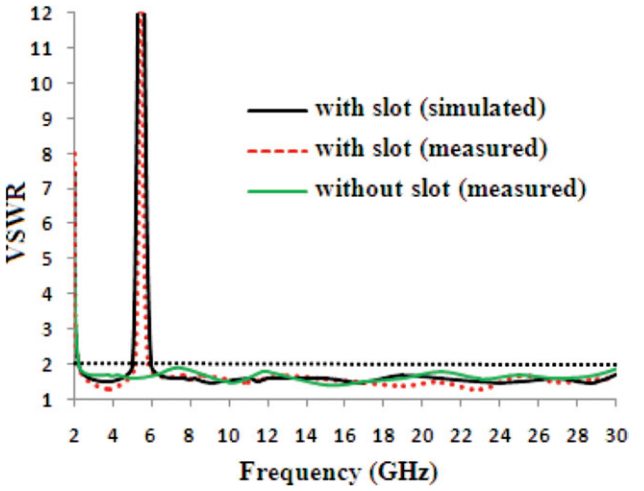

Figure 4 Comparison of simulated and measured VSWR results of the antenna. [Color figure can be viewed in the online issue, which is available at wileyonlinelibrary.com]

shows a slight shift because of the change in the size of the tuning stub. As such, for different values of "L_s" and "'W_s," the resonant curves have similar shape but, variation trend.

The optimum value is found to be $L_s = 6.2$ mm and $W_s = 9$ mm (Fig. 2) because, it provides the widest impedance bandwidth from 2.1 to 30 GHz for VSWR less than to 2, which is consistent for 2.4 GHz WLAN and UWB operations. Indeed, the wide bandwidths are due to the resonances introduced by the combination of the modified rectangular stub and the similar shaped slot. When proper dimensions (L_s and W_s) are selected, the resonant modes are shifted close to the antenna's fundamental resonant mode, resulting in high impedance bandwidth for 2.4 GHz WLAN and UWB systems.

2.3. Effect of Slot in the Stub

The influence of slot embedded on the tuning stub is also investigated for notch band function. Figure 3 shows the simulated VSWR of the proposed antenna with different length "L_t" of the slot (its width is kept at 0.4 mm).

From the figure, it is observed that the length of the slot line in the stub determines the frequency range of the notched band. As "L_t" increases, the center frequency of the notched band shifts toward the lower frequency. With the increasing of "L_t" from 17 to 18 mm, the center frequency shifts from 5.62 to 5.38 GHz. Thus, when "L_t" is 17.5 mm, the notch band is from 5.1 to 5.9 GHz centered at 5.5 GHz. From this, it is concluded that the rejected band can be easily obtained by tuning the length of the slot introduced inside the stub, that is, when the length of the slot is equal to quarter wavelength of the notch band center frequency, the notch band is from 5.1 to 5.9 GHz. This means that the slot cut made on the stub prohibits the current flow at the notch frequency, giving maximum attenuation at the notch band center frequency. This phenomenon is similar to the behavior of a quarter wave open circuited stub. Finally, the antenna covers a wide bandwidth from 2.1 to 30 GHz with 5 GHz notch band.

3. SIMULATION AND EXPERIMENTAL RESULTS

3.1. VSWR versus Frequency

The designed antenna is modeled and simulated using momentum software package of the Advanced Design System and CST

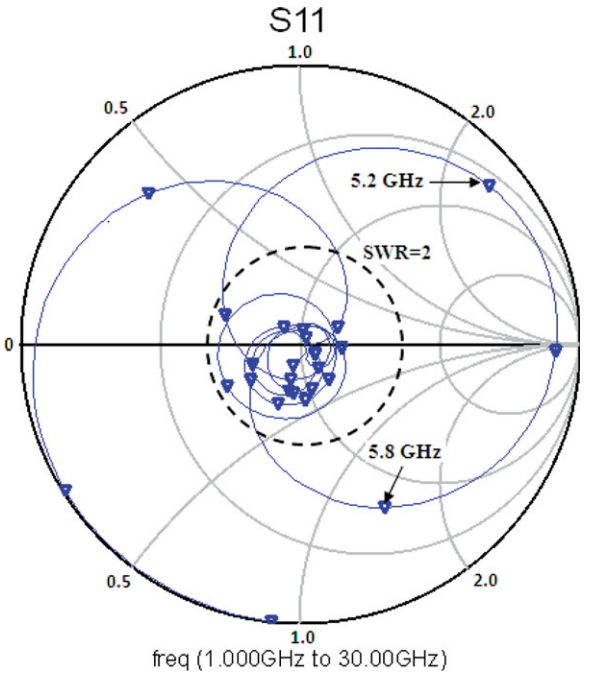

Figure 5 Simulated input impedance on Smith chart. [Color figure can be viewed in the online issue, which is available at wileyonlinelibrary.com]

microwave studio. Based on the optimized dimensions, the proposed antenna was fabricated as shown in Figure 2 and VSWR versus frequency of the antenna was measured with a HP8722ES Vector network analyzer. Figure 4 shows the measured VSWR of the CPW fed slot antenna as well as simulation results. Result of the antenna without slot in the stub is also given for comparison. Simulation and measurement results show that the proposed antenna performs well over the wide band of frequencies ranging from 2.1 to 30 GHz for VSWR less than 2, which covers the 2.4 GHz WLAN and UWB bands with notch-band from 5.1 to 5.9 GHz. Moreover, the simulated and measured results are fairly consistent with each other throughout the operating frequencies. Hence, basic agreements are achieved between the simulated and the measured results. The discrepancies between them may be caused by the result of the cable leakage current on the coaxial cable that is used to feed the

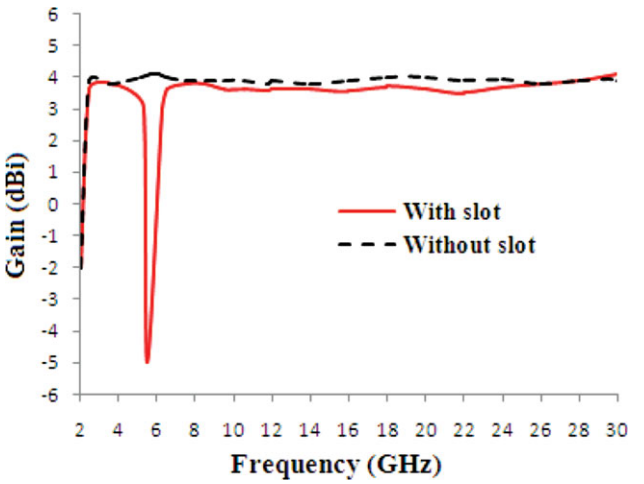

Figure 7 Peak gain of the proposed antenna. [Color figure can be viewed in the online issue, which is available at wileyonlinelibrary.com]

antenna prototype in the measurements, the fabrication error and soldering effects of SMA connector. Figure 5 shows the resonance and impedance matching over the operating frequency, that is, it confirms the impedance matching performance between 2.1 and 30 GHz with notch band function (5.1–5.9 GHz). The impedance curve spirals out of the VSWR = 2 circle between 5.1 and 5.9 GHz, showing high input impedance at notch frequency, which is produced by the slot cut on the tuning stub. The curve inside the VSWR circle indicates the optimum impedance bandwidth for the operating frequency from 2.1 to 30 GHz.

3.2. Radiation Patterns and Gain

The radiation patterns and gain measurements are performed inside the anechoic chamber of Antenna Laboratory. The radiation characteristics of the antenna were experimentally investigated across the impedance bandwidth from 2.1 to 30 GHz.

Figure 6 shows the measured radiation patterns at 2.4, 15, and 26 GHz in the two principal planes, namely the *x–z* and *x–y* planes. It can be seen that the radiation patterns in *x–y* plane are nearly omnidirectional for the three frequencies and the patterns in *x–z* plane are of figure eight patterns. Radiation patterns are acceptable over the whole 2.4 GHz WLAN/UWB bandwidth.

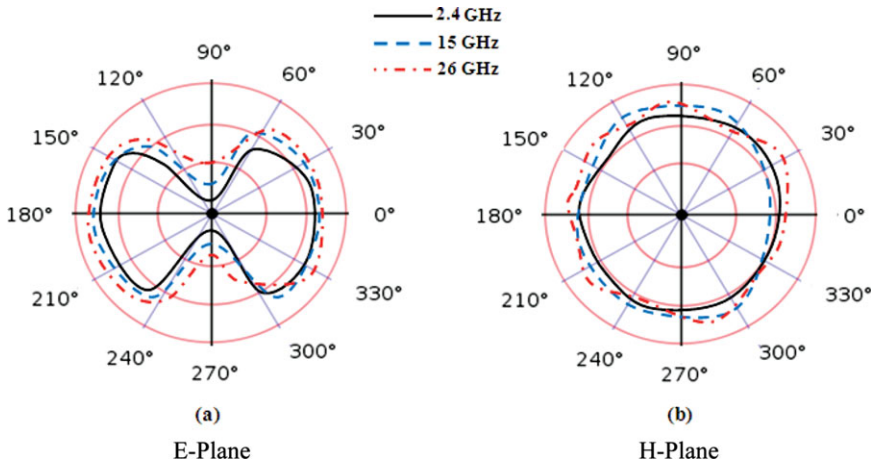

Figure 6 Radiation patterns at (a) 2.4 GHz, (b) 15 GHz, and (c) 26 GHz. [Color figure can be viewed in the online issue, which is available at wileyonlinelibrary.com]

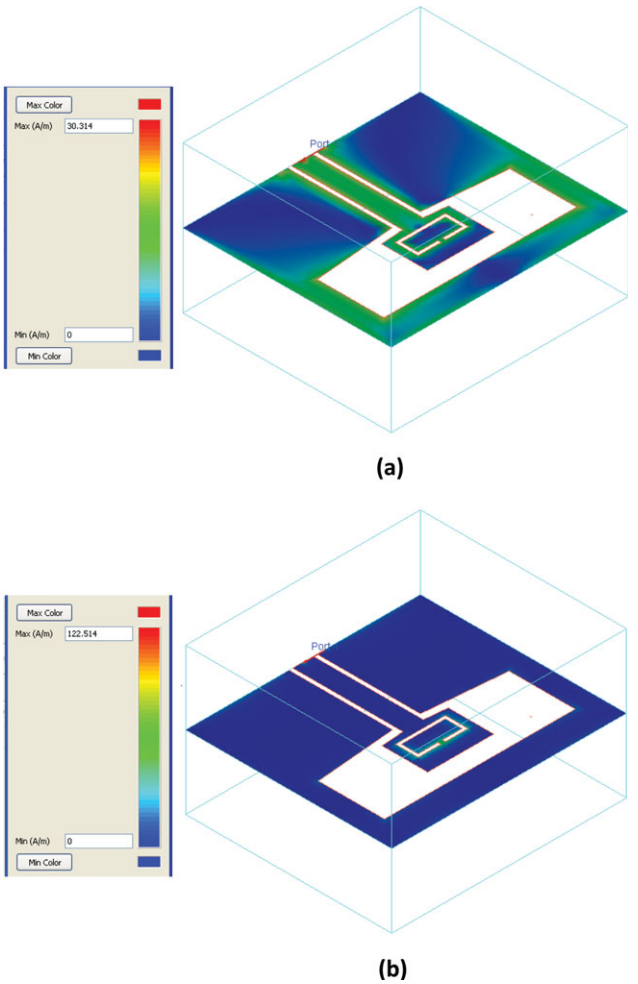

Figure 8 Simulated current distributions on the antenna (a) at 2.4 GHz and (b) at 5.5 GHz. [Color figure can be viewed in the online issue, which is available at wileyonlinelibrary.com]

Also, it is observed that radiation patterns at other frequencies out of the notched frequency band are about stable, suggesting the usefulness of the antenna in the entire band.

The gain versus frequency of the proposed antenna is also found to be suitable for the 2.4 GHz WLAN and UWB applications. Figure 7 shows the measured gain versus frequency of the proposed antenna. Gain of the antenna without slot on the stub is also included for comparison. For the antenna without slots, the peak gain is relatively constant over the band from 2.1 to 30 GHz. But, for the proposed antenna, antenna gain decreases drastically at the frequency of 5.5 GHz due to the frequency notched function and the peak gain is nearly constant outside the notched band from 2.1 to 30 GHz. Thus, the antenna exhibits a stable gain across the operation band. These factors demonstrate the band notched function of the proposed antenna.

3.3. Current Distributions

The surface current distribution has been studied using ADS simulation tool. The current distribution of the proposed antenna is obtained by accounting the optimal design parameter values. Figure 8 shows the simulated current distributions at frequencies 2.4 and 5.5 GHz. At frequency 2.4 GHz, the maximum current flow occurs and the antenna radiates signal [Fig. 8(a)]. But, at the notch band centre frequency 5.5 GHz, current is concentrated around the edge of the slot on the modified rectangular stub while there is almost no current at the feeding point. The electric currents concentrate around the slot structure in correspondence with the center frequency of the unwanted band and it prohibits the current flow at that frequency, giving maximum attenuation. The current distributed around the slot on the stub results in band stop effect. Thus, it shows the effect of the slot on the antenna performance at the notched frequency [Fig. 8(b)].

4. CONCLUSION

A compact design and construction of a wide slot antenna fed by a CPW has been developed for multifunctional communication systems. Detailed simulations and experimental investigations were performed to understand the behavior of the proposed slot antenna for 2.4 GHz WLAN and ultrawideband systems. The antenna has a modified rectangular stub with CPW feed technique, which improves the impedance matching for 2.4 GHz WLAN and UWB operations. Band notch function was also explored. Prototype of the proposed antenna has been fabricated and measurement was done. The antenna has VSWR value less than 2 between 2.1 and 30 GHz. The performance analysis such as the radiation patterns, antenna gain and current distribution was discussed. It shows better performance over the required bandwidth for use in multifunctional communication systems.

REFERENCES

1. FCC report and order for part 15 acceptances of ultra wideband (UWB) systems from 3.1–10.6 GHz, Washington, DC, 2002.
2. X. H. Wu, Z.N. Chen, and M.Y.W. Chia, Note on antenna design in UWB wireless communication systems, In: IEEE Conference on Ultra Wideband Systems and Technologies, 16–19 November 2003, pp. 503–507.
3. G. Vonder Mark, S. Lu, I. Korisch, L.J. Greenstein, and P. Spasojevic, Diamond and rounded diamond antennas for ultra wide-band communications, IEEE Antennas Wireless Propag Lett 3 (2004), 249–252.
4. Y. Ren and K. Chang, An annular ring antenna for UWB communications, IEEE Antennas Wireless Propag Lett 5 (2006), 275–276.
5. K. Kiminami, A. Hirata, and T. Shiozawa, Double-sided printed bow-tie antenna for UWB communications, IEEE Antennas Wireless Propag Lett 3 (2004), 152–153.
6. C.Y. Huang and W.C. Hsia, Planar Elliptical Antenna for Ultra-wideband Communications, Electron Lett 41 (2005), 296–297.
7. S.W. Su, K.L. Wong, and C.L. Tang, Ultra-wideband square planar monopole antenna for IEEE 802.16a operation in the 2–11 GHz band, Microwave Opt Technol Lett 42 (2004), 463–466.
8. Y.F. Liu, K.L. Lau, Q. Xue, and C.H. Chan, Experimental studies of printed wide-slot antenna for wide-band applications.IEEE Antennas Wireless Propag Lett 3 (2004), 273–275.
9. J.-Y. Sze, C.-I.G. Hsu, and J.-J. Jiao, CPW-fed circular slot antenna with slit back-patch for 2.4/5 GHz dual-band operation, IEE Electron Lett 42 (2006).
10. W.-S. Chen and F.-M. Hsieh, Broadband design of the printed triangular slot antenna, In: IEEE Antennas and Propagation Society International Symposium, Monterey, CA, Vol. 4, June 2004, pp.3733–3736.
11. J.-S. Chen, Dual-frequency annular-ring slot antennas fed by CPW feed and microstrip line feed, IEEE Trans Antennas Propag 53 (2005), 569–571.
12. R. Garg, P. Bhartia, I.J. Bahl, and A. Ittipiboon, Microstrip antenna design handbook, Artech House, Norwood, MA, 2001.
13. K.L. Wong, Compact and broadband microstrip antennas, Wiley, Hoboken, NJ, 2002.
14. G. Kumar and K.P. Ray, Broadband microstrip antennas, Artech House, Boston, 2003.
15. R. Chair, A.A. Kishk, and K.F. Lee, Ultrawide-band coplanar waveguide-fed rectangular slot antenna, IEEE Antennas Wireless Propag Lett 7 (2004), 227–229.

16. T.A. Denidni and M.A. Habib, Broadband printed CPW-fed slot antenna, IEE Electron Lett 42 (2006).
17. P.L. Liang and X. Chen, Study of printed elliptical/circular slot antennas for ultrawideband applications communication, IEEE Trans Antennas Propag 54 (2006), 1670–1675.

THEORETICAL LIMITS ON MINIATURIZATION OF DIRECTIONAL COUPLERS DESIGNED AS A CONNECTION OF TIGHTLY COUPLED AND UNCOUPLED LINES

Krzysztof Wincza and Slawomir Gruszczynski
AGH University of Science and Technology, Faculty of Electrical Engineering, Automatics, Computer Science and Electronics, 30-059 Cracow, Poland; Corresponding author: slawomir.gruszczynski@agh.edu.pl

Received 10 May 2012

ABSTRACT: *The problem of miniaturization of coupled-line directional couplers designed as a connection of tightly-coupled and uncoupled sections has been comprehensively investigated for the first time. It has been proven that in such couplers the stronger coupling is available in the structure, the greater miniaturization is achieved. A novel approach allowing for theoretical analysis of such couplers has been proposed. Moreover, a special case has been considered, in which couplers are designed with the use of a single section of uncoupled lines placed in the middle of a tightly-coupled section. The proposed approach has been utilized for derivation of theoretical limits describing the maximum achievable minimization of the overall electrical length of couplers designed as a connection of coupled and uncoupled lines. The theoretical analyses have been confirmed by the measurements of two different directional couplers designed with the use of the proposed approach.* © 2012 Wiley Periodicals, Inc. Microwave Opt Technol Lett 55:223–230, 2013; View this article online at wileyonlinelibrary.com. DOI 10.1002/mop.27233

Key words: *coupled lines; broadband directional couplers; tightly coupled lines; ideal coupled-line sections; miniaturized directional couplers*

1. INTRODUCTION

Coupled-line directional couplers are well-known networks often used in contemporary microwave engineering. This is due to the fact that they offer broader bandwidth than branch-line couplers. One prominent issue of coupled-line directional coupler is how to miniaturize it, important especially at lower frequency ranges. Although coupled-line directional couplers require smaller occupied area than branch-line couplers, the problem of coupled-line couplers' miniaturization is still of interest. One of the possible approaches for directional couplers' miniaturization is to use a lumped-element technique. Initially, such a technique has been used for miniaturization of couplers composed of sections of transmission lines [1–5]. Subsequently, the possibility of coupled-line directional couplers' miniaturization has been approached with the lumped-element technique. Exemplary designs of such networks can be found in [6] and [7]. In both cases, however, a single-section equivalent circuit has been assumed which result in poor performance of the couplers. Other examples of coupled-line couplers designed with the use of a lumped-element technique can be found in [8] and [9], in which two-subsection equivalent circuits have been assumed. In [10], we have shown the analysis of coupled-line couplers designed using a quasi-lumped-element technique. As it has been shown the couplers' performance strongly depends on the number of subsections. The lower number of subsections is chosen, the worse return losses and isolation are achieved, and also the bandwidth of the designed coupler is reduced [10]. In the presented examples a three-section equivalent circuits have been chosen to achieve good couplers' performance. On the other hand, it is known that a single-section coupled-line directional coupler can be designed as a connection of coupled-line sections having different electrical lengths and coupling coefficients. As it has been shown in [11] such a solution provides greater design flexibility. Moreover, when the center subsection is substituted by two uncoupled transmission lines, the overall coupler length can be reduced at the expense of slight bandwidth reduction [12].

In this letter, we present a comprehensive analysis of directional couplers designed as a connection of tightly-coupled and uncoupled sections that focuses on the maximum achievable miniaturization of such couplers. The proposed method of analysis of such networks is based upon the assumption that the short tightly-coupled section has to realize the overall mutual capacitance and inductance that is needed for achieving the nominal coupling of the designed coupler. With this assumption the electrical length of the tightly-coupled section can be found, and further, the electrical length of uncoupled lines can be calculated assuming that the uncoupled lines have to realize the missing self-capacitance and self-inductance of the initial coupler. It is shown that such an approach is appropriate when tightly-coupled and uncoupled sections are equally distributed along the coupler, i.e., assuming infinite number of subsections. Moreover, in this case, the performance of the coupler is identical to the conventional one—i.e., single 90°-long coupled-line section—featuring the same bandwidth, ideal impedance match, and isolation. Subsequently, a special case is considered, in which two uncoupled lines are placed in the middle of a tightly-coupled section. In this case, the effect of bandwidth reduction occurs, as it was shown in [12], and for such a case more accurate method of analysis is proposed in this letter. It has to be underlined, that although the accurate method of analysis of the network composed of uncoupled lines placed in the middle of a coupled-line section is shown in [12], the approach proposed in this letter allows for deriving analytical expressions on the required electrical lengths of both tightly-coupled and uncoupled sections. Subsequently, the proposed approach has been utilized for the purpose of investigating the miniaturization limits of such networks. The limits have been derived for both considered cases. The theoretical analysis has been confirmed by the measurements of two manufactured couplers designed with the use of the proposed method.

2. THEORETICAL ANALYSIS—GENERAL CASE

Figure 1 presents a single-section coupled-line directional coupler described by the characteristic impedance Z_0, nominal coupling k_{nom}, electrical length $\Theta_{\mathrm{nom}} = 90^\circ$, and its equivalent circuit composed of n identical sections. Each section consists of two tightly-coupled lines described by the characteristic impedance Z_0, coupling k_{max}, and electrical length $\Theta_{\mathrm{cpl}}/2n$, between which, two uncoupled lines are inserted (described by the characteristic impedance Z_0 and electrical length Θ_{trl}/n). It is obvious from Figure 1 that the overall length of tightly-coupled sections is equal Θ_{cpl}, whereas the overall length of uncoupled lines is equal Θ_{trl}. At first, let us notice that the mutual capacitance and mutual inductance per unit length of two uncoupled